PRAMANA — journal of physics
© Indian Academy of Sciences
Vol. 60, No. 1
January 2003
pp. 99–107

Operational characteristics and power scaling of a transverse flow transversely excited CW CO_2 laser

JAI KHARE, R SREEDHAR, C P PAUL, T REGHU and A K NATH*
Industrial CO_2 Laser Section, Centre for Advanced Technology, Indore 452 013, India
*Email: aknath@cat.ernet.in

MS received 17 June 2002; revised 30 August 2002

Abstract. Transverse flow transversely excited (TFTE) CO_2 lasers are easily scalable to multi-kilowatt level. The laser power can be scaled up by increasing the volumetric gas flow and discharge volume. It was observed in a TFTE CW CO_2 laser having single row of pins as an anode and tubular cathode that the laser power was not increasing when the discharge volume and the gas volumetric flow were increased by increasing the electrode separation keeping the gas flow velocity constant. The discharge voltage too remained almost constant with the change of electrode separation at the same gas flow velocity. This necessitated revision of the scaling laws for designing this type of high power CO_2 laser. Experimental results of laser performance for different electrode separations are discussed and the modifications in the scaling laws are presented.

Keywords. CO_2 laser; transverse flow; dc excitation; scaling laws.

PACS Nos 42.55.Lt; 42.60.By; 42.60.Lh

1. Introduction

Transverse flow transversely excited CW CO_2 laser with multiple pins discharge electrodes is one of the simple designs to construct a multi-kilowatt CO_2 laser [1–4]. In a convective cooled laser the laser power scales up with the laser gas flow velocity as

$$P_L = (\eta/\eta - 1)\rho C_p \Delta T vwL \tag{1}$$

$$P_L \approx 120M^\bullet. \tag{2}$$

where η is the electro-optic efficiency, ρ the laser gas density, C_p the specific heat of the laser gas, ΔT the rise in the laser gas temperature, v the gas flow velocity, w the discharge width, L the discharge length (figure 1) and $M^\bullet$ the mass flow rate of the gas. This is with the assumption that maximum electrical input power, limited by the bottlenecking at the lower laser level can be dissipated in a stable and uniform discharge. In fast gas flow lasers, where the gas residence time is too small for any discharge instability to grow and deteriorate the discharge quality, the input power is limited by the rise of gas temperature.

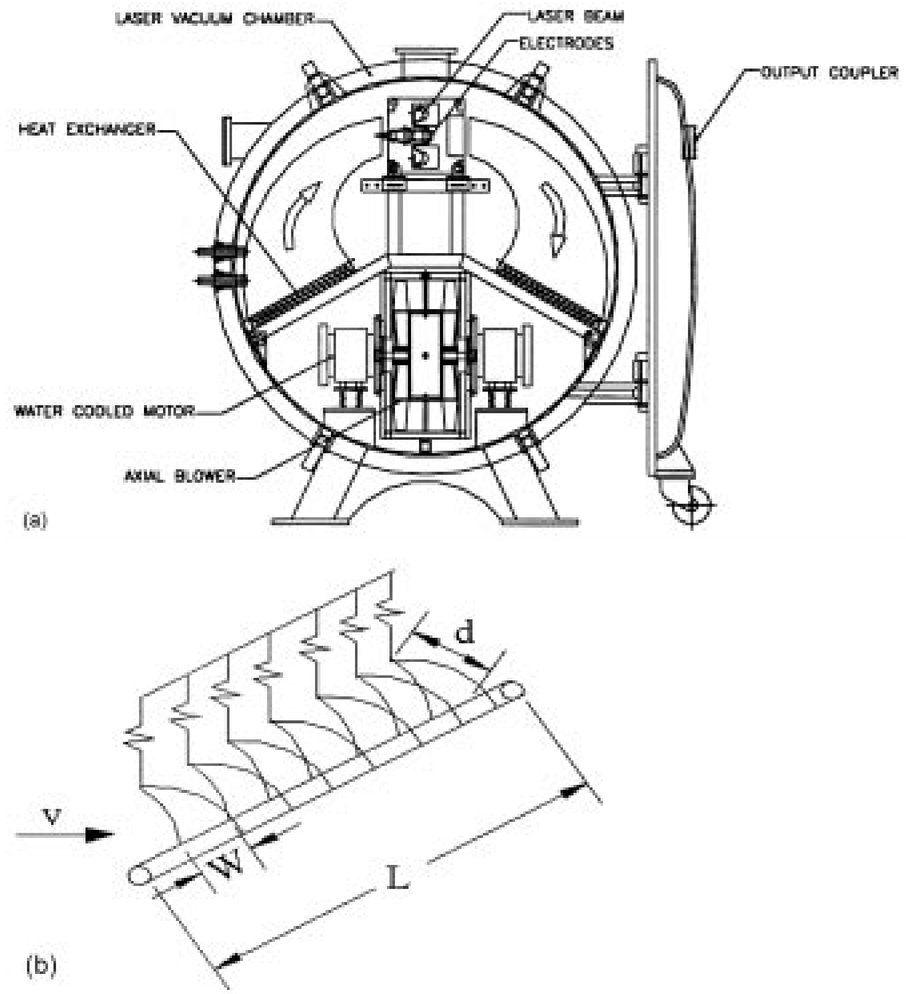

Figure 1. (**a**) Schematic diagram of a transverse flow transversely excited CW CO_2 laser. (**b**) Schematic diagram of the resistance ballasted multiple pins anode and tubular cathode.

Under such conditions the authors had earlier derived an expression for the discharge width and length for any desired laser power and gas flow velocity from eq. (1) as expressed in the following equation [5].

$$w\ (\mathrm{cm}) = 0.04[P_{\mathrm{L}}\ (\mathrm{W})]^{1/2} \tag{3}$$

$$L\ (\mathrm{cm}) = 1.4 \times 10^4 [P_{\mathrm{L}}(\mathrm{W})]^{1/2} [V\ (\mathrm{cm/s})]^{-1}. \tag{4}$$

We developed a TFTE laser system having a pair of anodes and a common tubular cathode [3] and operated with different electrode gaps and gas flow velocities. The laser head and the electrode configuration are schematically shown in figure 1. One would expect that the discharge voltage will increase with the increase of discharge gap, but it was almost constant for different electrode separations in the present experimental range at a constant gas flow velocity. The gas mass flow was increased with the increase of electrode gap at the same gas velocity, and according to eq. (2) the laser power should have increased. But the maximum laser power that can be obtained by maintaining the uniform and stable discharge remained almost constant. However, when the gas flow velocity was increased, the discharge voltage and the laser power both increased. It indicated that in the present laser design the laser power had a stronger dependence on the gas flow velocity rather than on the volumetric or mass flow rate. Since the expressions for discharge width and length given by eqs (3) and (4) are derived based on the laser power scaling with the volumetric/mass flow given by eq. (2) these will require modification for designing lasers of larger volumes and higher powers.

It was also observed that the optimum laser gas mixture for maximum laser power at different electrode gaps was not the same. The partial pressure of nitrogen in the optimum gas mixture was higher for smaller electrode separation. Kuzumoto *et al* [6] had reported very high partial pressure of nitrogen in optimum laser gas mixture of a transverse-flow CW CO_2 laser excited by the silent discharge (SD). They found that the reduced electric field across SD was more than the electric field in a conventional dc glow discharge. They estimated the excitation efficiency to N_2 vibration levels in SD with high N_2 concentration ($\approx 60\%$) and found it the same as that in dc discharge. Chang *et al* [7] had reported unusual optimum laser mixture $CO_2:N_2:He = 1:22:5$ in a fast axial flow CO_2 laser excited by SD. They carried out experiments in fast flow systems with different electrode separations excited by dc, SD and rf discharge, and concluded that a CO_2 laser with a short distance between electrodes and a low gas pressure should require less helium and more nitrogen. However, in our laser with similar electrode separation, partial pressure of helium in the optimum laser gas mixture was comparable to that of nitrogen.

In this paper we present the dependence of discharge current and voltage, input power density and the laser power on the discharge width and also the qualitative explanations for the experimental observations. Based on these results we modify the scaling laws also.

2. Experimental results

Experiment was carried out in a pulser-sustained TFTE CW CO_2 laser whose construction details are described elsewhere [4]. It had a pair of anodes and a common tubular cathode (figure 1). Each anode consisted of 90 resistance-ballasted pins made of 3 mm diameter stainless steel and distributed at equal distance over 90 cm discharge length. Total discharge length was 180 cm. A pair of contra-rotating axial fans circulated the laser gas through the discharge zone and the heat exchangers. Population inversion was produced by a pulser-sustained dc discharge. The laser power was extracted with a folded stable resonator formed with a near 100% reflecting concave mirror of 15 m radius of curvature, a rooftop mirror for folding the beam and a plane ZnSe output coupler of 50% reflectivity. Laser was operated with three different electrode separations. The optic axis was in the downstream at a distance equal to about one-half of the electrode separation, where the laser power obtained was the maximum. Even though the anode consisted of a single row of pins across the direction of gas flow and the cathode was a 12 mm diameter tube, the

Table 1. Discharge length $= 92 \times 2 = 180$ cm, gas pressure $= 45$ mbar.

Electrode gap (cm)	Discharge current (A)	Discharge voltage (V)	$CO_2 : N_2 : He$	Laser power (kW)	Input power density (W/cc)	Efficiency (%)
Gas flow velocity = 35 m/s						
2.5	24	1330	1 : 10 : 9	3.2	33	10
3.0	23	1360	1 : 8 : 11	3.2	23	10
3.5	22	1390	1 : 6.5 : 12.5	3.5	17	11.4
Gas flow velocity = 45 m/s						
3.0	24	1430	1 : 8 : 11	5.0	26	14.5
Gas flow velocity = 50 m/s						
4.2	25	1600	1 : 6 : 13	6.5	16	16.2

Excitation: Pulser sustained dc discharge. Pulser characteristics: Peak voltage= 12 kV; repetition frequency = 3.3 kHz, pulse duration =∼500 ns.

laser beam formed in the downstream was of nearly square cross-section. The size was about 85% of the electrode separation. In the first set of experiments, the gas flow was kept constant at ∼35 m/s and laser power was maximized for three different electrode separations. It was observed that the maximum discharge current, discharge voltage and the laser power remained almost constant for different electrode gaps. However, the optimum gas mixtures for the maximum laser power were different for different electrode gaps. The nitrogen partial pressure was more when the electrode gap was smaller. The maximum discharge current, discharge voltage, laser power, optimum laser gas mixture and other parameters are presented in table 1. It was difficult to estimate the discharge cross-section in this type of discharge geometry. Therefore, the discharge cross-section was assumed to be equal to the laser beam size and the input power density mentioned in the table was estimated accordingly. In other sets of experiments the gas flow velocity was increased. The laser power and the electro-optic efficiency were increased with the increase of gas velocity. These are also tabulated in table 1.

We have obtained the maximum 6.5 kW laser power with about 16% electro-optic efficiency in a multimode laser beam of 35×36 mm size. Figure 2 shows the beam pattern taken on ceramic brick.

From the above experimental results the following observations can be made:

1. Laser power and electro-optic efficiency were increased with the increase of gas flow velocity.
2. One would expect that the discharge voltage would scale up with the electrode gap and the discharge electrical field would remain constant to maintain the same discharge current. But the discharge voltage did not increase proportional to the increase in electrode gap. However, it was increased when the gas flow velocity was increased.
3. Maximum discharge current that can be put without the onset of discharge instability was reduced slightly with the increase of electrode gap and increased with the increase of gas velocity.
4. At the same gas flow velocity the laser power was almost unchanged with the increase of electrode gap, though the latter increased the discharge volume and the volumetric gas flow.

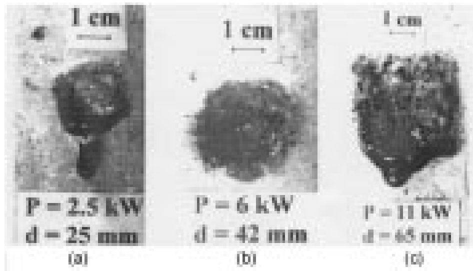

Figure 2. Laser beam pattern on ceramic bricks for different electrode separation d and laser power P. (**a**) $d = 25$ mm, $P = 2.5$ kW; (**b**) $d = 42$ mm, $P = 6$ kW; (**c**) $d = 65$ mm, $P = 11$ kW.

5. Input power density varied inversely proportional to nearly square of the electrode gap at the same gas flow velocity.
6. Partial pressure of nitrogen in the optimum laser gas mixture reduced and that of helium increased with the increase of electrode gap.

In the following section we present qualitative explanation for these observations.

3. Discussions

Enhancement of laser power and efficiency with the increase of gas flow velocity can be easily understood. Increase in gas flow velocity reduces the rise in gas temperature. This in turn, increases the laser gain for the same input power and also reduces the decay rate of the population inversion by collisions [8]. Both these factors contribute in the enhancement of laser power and efficiency with the increase of gas flow velocity.

The maximum discharge current can be assumed to be almost constant (within $\pm 5\%$) for different electrode gaps and flow velocities. It was observed that the maximum current was limited by the onset of discharge instability. Maximum discharge current through each pin electrode was limited within 120–140 mA. It would depend, among other factors, on the electric field around the tip of the pin and the gas flow velocity. As the input power density for different electrode gaps was different, the rise in gas temperature would also be different. From this it can be concluded that the discharge instability is not caused by the rise in laser gas temperature, but it is caused by the ionization instability [9].

The growth of electron by ionization with time can be given by

$$n(t) = n(0)\exp(\alpha_{\rm i} N_{\rm a} t) \tag{5}$$

where $\alpha_{\rm i}$ is the ionization rate constant and is a function of $E/N_{\rm a}$, E the discharge electric field, $N_{\rm a}$ the gas number density and $n(0)$ the initial electron density.

The maximum growth of current within the gas residence time should be almost the same for different electrode gaps to cause discharge instability. Therefore, $\alpha_{\rm i} N_{\rm a} \tau =$ constant, where τ is the gas residence time, which can be defined as $\tau =$ discharge width along the direction of gas flow/gas flow velocity $= w/v$.

Assuming $\alpha_{\rm i}$ to be proportional to $E/N_{\rm a}$ [10], we get

$$E \propto v/w, \text{ or for a constant } v, E \propto 1/w. \tag{6}$$

It has been observed that $w \cong$ electrode gap d (figure 1) and from eq. (6) this leads to $Ed =$ discharge voltage $V =$ constant for the constant gas flow velocity. This substantiates the experimental observation.

Since total input power $= VI$ remains almost constant for different electrode gaps at constant gas flow velocity, the laser output power is also constant, though the gas volumetric flow gets increased due to increase in electrode gap.

The input power density, $P_{\text{in}} = VI/Ldw$.

As we have seen that V and I are constant for a given discharge length L, this makes

$$P_{\text{in}} \propto 1/d^2.$$

This explains the experimental observation mentioned in observation 5 in §2.

Since the discharge voltage remained almost constant, the electric field was reduced with the increase of electrode gap. The excitation efficiency of N_2 vibration level depends upon the average electron energy in the discharge, which in turn depends on E/N_{a} and the gas mixture. It is well established that the average electron energy increases with the decrease of N_2 partial pressure and increase of He partial pressure in a laser gas mixture for a given E/N_{a} [11]. Since the electric field reduced with the increase of the electrode gap, the partial pressure of N_2 had to be reduced with the increase of the electrode gap and that of He had to be increased to maintain the same average electron energy for the maximum N_2 excitation efficiency. Solving the Boltzmann equations [12] we calculated the electron energy distribution and the average electron energy for different optimum laser gas mixtures and discharge electric fields. Figure 3 shows the electron energy distributions in 1 : 10 : 9, 1 : 8 : 11 and 1 : 6.5 : 12.5 gas mixtures at their respective optimum electric fields, i.e., 532 V/cm, 453 V/cm and 397 V/cm corresponding to different electrode separations. The electron energy distributions in these three cases are almost the same. Figure 4 shows the electron energy distributions for 1 : 10 : 9 gas mixture at the three above mentioned electric fields. The distributions are not the same. The average electron energies for different gas mixtures and electric fields are presented in table 2. The gas mixture for which the average electron energy was about 1.2 eV was optimum for that electrode separation. This is quite close to the value reported by Kuzumoto *et al* [6]. The optimum

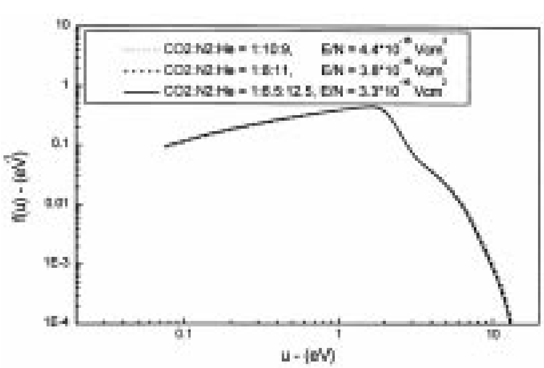

Figure 3. Electron energy distribution functions for different gas mixtures and E/N optimum for different electrode separations.

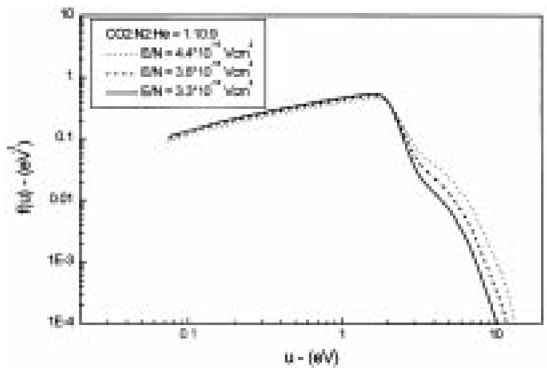

Figure 4. Electron energy distribution function for a typical gas mixture at different E/N.

Table 2. Average electron energy for different gas mixtures and discharge electric fields corresponding to different electrode gaps.

Electric field	532 V/cm	453 V/cm	397 V/cm
Electrode gap	2.5 cm	3.0 cm	3.5 cm
E/N	4.4×10^{-16} V cm^2	3.8×10^{-16} V cm^2	3.3×10^{-16} V cm^2
Gas mixture $CO_2 : N_2 : He$	Average electron energy (eV)		
1 : 10 : 9	1.22	1.07	0.97
1 : 8 : 11	1.39	1.20	1.07
1 : 6.5 : 12.5	1.55	1.33	1.18

mixture ratios of laser gases reported by Chang *et al* [7] in the dc discharge with different electrode separations and gas pressures are also in the similar range as observed in our system. These calculations confirm that the variation in the optimum laser gas mixture for different electrode separations was to maintain the same electron energy distribution and average electron energy for which the N_2 excitation was the maximum.

4. Scaling laws

In the present laser the following scaling laws seem to hold:

1. Discharge voltage is almost independent of electrode gap for the same gas flow velocity.
2. Discharge voltage increases with the gas flow velocity.
3. Discharge current is proportional to the number of pin electrodes, i.e., discharge length, and input power density is inversely proportional to square of the discharge gap.

Since the laser power did not increase with the increase of electrode gap, in order to scale up the laser power we have to not only increase the electrode gap but also the flow velocity.

For a small discharge width wherein P_{in} is limited by the rise in the gas temperature, i.e., the thermal bottlenecking, the discharge length L and width w can be estimated using eqs (3) and (4). But for the larger electrode gaps wherein P_{in} is limited by ionization instability, and the maximum rise in gas temperature is less than the optimum limit ($\sim 250\,^{\circ}$C), eq. (4) will not provide the correct discharge length required for the desired laser power. While the electrode gap $d \approx w$ can be determined by eq. (3), we will need to modify the relationship between the discharge length and the laser power for the higher power lasers. Based on the present experimental results of the variation of discharge voltage with the flow velocity an empirical relation between the number of anode pins n and the maximum current in Ampere that can be passed through each pin i, the gas flow velocity v and the desired laser power P_L is obtained as the following:

$$n \cong 20P_L(\mathrm{W})[i\ (\mathrm{A})v\ (\mathrm{cm/s})]^{-1}.$$

The constant factor in the right-hand side only gets modified for different laser designs and corresponding discharge voltage.

Though the anode is made of discrete pins, the discharge initiated from adjacent pins gets overlapped along the optic axis in the downstream of gas flow. Thus,

$$\text{The discharge length } L = nl, \qquad (10)$$

where l is the center-to-center distance between two adjacent pins.

L is calculated using both eqs (4) and (7) and is plotted in figure 5. For the practical design the higher value of L between the two obtained using eqs (4) and (7) should be considered. It is evident from figure 5 that a higher gas flow velocity is desired to design a more compact high power laser. We are developing a higher power CW CO_2 laser of 20 kW power level based on this design. In the initial experimentation we energized half of the discharge sections and obtained about 11 kW laser power with about 12% electro-optic efficiency. The burn pattern shown in figure 2c was produced by this laser beam. Performance characteristics of this laser will be reported later on.

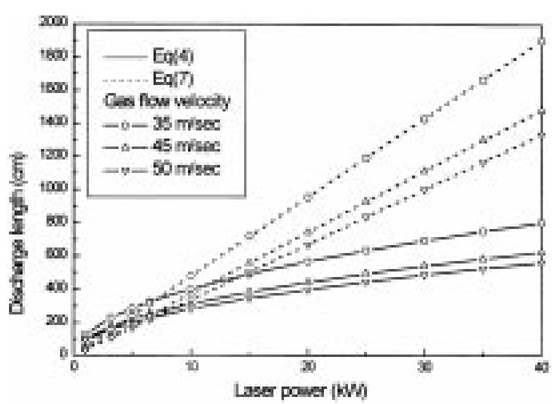

Figure 5. Discharge length calculated using eqs (4) and (7) vs. laser power for different gas flow velocities.

5. Conclusion

It can be concluded that the laser power in the TFTE CW CO_2 laser of the present design scales with the discharge length only for a constant gas flow velocity. This necessitates much larger discharge volumes for scaling up laser power at a constant flow velocity. For laser power to scale with the electrode separation the gas flow velocity should be also increased proportionally. In order to make the design more compact, special blowers, which can provide higher gas flow velocity through discharge zone have to be employed. The variation of the optimum laser gas mixture for different electrode separations is mainly to maintain the average electron energy in the discharge for most efficient excitation of nitrogen gas.

Acknowledgements

Authors wish to acknowledge with great appreciation the team members of the Industrial CO_2 Laser Section for their sincere and untiring efforts in developing indigenous high power CO_2 lasers.

References

[1] A K Nath, H J J Seguin and V A Seguin, *IEEE J. QE* **22**, 268 (1986)
[2] M Kasamatsu, S Shiratori and T Sato, *IEEE J. QE* **22**, 2026 (1986)
[3] K H Wu, *IEEE J. QE* **23**, 1981 (1987)
[4] A K Nath, L Abhinandan and P Choudhary, *Opt. Eng.* **33**, 1889 (1994)
[5] A K Nath and V S Golubev, *Pramana – J. Phys.* **51**, 463 (1998)
[6] M Kuzumoto, S Ogawa and S Yagi, *J. Phys. D: Appl. Phys.* **22**, 1835 (1989)
[7] S H Chang, C C Cheng, M F Chang, H S Tsai and H P Liu, *Jpn. J. Appl. Phys.* **39**, 82 (2000)
[8] M Kuzumoto, M Tanaka and S Yagi, *IEEE J. QE* **27**, 471 (1991)
[9] G A Abilsitov, E P Velikhov, V S Golobev and F Lebedev, *Sov. J. QE* **11**, 1535 (1981)
[10] N Motsuoka, S Yamaguchi, K Nonri and T Fujoka, *Jpn. J. Appl. Phys.* **38**, 6340 (1999)
[11] O P Judd, *J. Appl. Phys.* **45**, 4572 (1974)
[12] K Smith and R M Thomson, *Computer modeling of gas lasers* (Plenum Press, New York, 1978)